Tohoku J. Exp. Med., 2024, **263**, 249-259

Gastrodin Regulates Cardiac Arrhythmia by Targeting the Gap Junction Alpha-1 Protein after Ischemia-Reperfusion

Juan Huang,[1,*] Guoqu Jia,[1,*] Qi Wu,[1] Hong Yang,[1] Chunmei Liu[1] and Songjie Bi[1]

[1]Department of Cardiovascular Medicine, The Second Affiliated Hospital of Chengdu Medical College, China National Nuclear Corporation 416 Hospital, Chengdu, Sichuan, China

The effects of Gastrodin (GD) on cerebral ischemia stimulated researchers to investigate its possible role in the progression of arrhythmia associated with cardiac ischemia-reperfusion (IR) damage in rats. 40 Sprague-Dawley rats were divided into four groups: Sham, Model, GD 50 mg/kg, and GD 100 mg/kg. Myocardial ischemia (MI) was caused by the procedure of ligating the left coronary artery, followed by reperfusion. Heart rate (HR), mean arterial pressure (MAP), and rate pressure product (RPP) in rats were assessed before and after ischemia and reperfusion, as well as cardiac arrhythmia in experimental rats. The I/R damage was evaluated by measuring levels of Na^+-K^+ATPase and Ca^{2+}-Mg^{2+}ATPase, Creatine Kinase-MB (CK-MB), Cardiac Troponin I (cTnI), Gap Junction *α*-1 (GJ*α*-1), Phospho-GJ*α*-1/total-GJ*α*-1, Kir2.1, Bax, Bcl-2, and oxidative indicators. MGL's Autodock and Vina programs were used for in silico docking studies to identify possible interactions between GJ*α*-1 and Gastrodin. The animals in the model group expressed a substantial decrease in HR, MAP, and RPP compared to the Sham group. GD-treated rats revealed slightly higher values compared to the model group. Expression of CK-MB and cTnI was reduced, and Na^+-K^+ATPase and Ca^{2+}-Mg^{2+}ATPase expression was increased on GD pre-conditioning. Phospho-Cx43/total-Cx43 ratio and Bax expression were increased, whereas GD reduced Bcl-2 expression. In silico molecular docking studies suggested the potential binding of GD with the GJ*α*-1 protein, thus confirming the *in vivo* results. GD corrected the arrhythmia in rats subjected to I/R injury by increasing Na^+-K^+ATPase and Ca^{2+}-Mg^{2+}ATPase expression, targeting GJ*α*-1, and modulating the expression of Kir2.1.

Keywords: cardiac arrhythmia; Gap Junction alpha -1; Gastrodin; myocardial ischemia; reperfusion injury
Tohoku J. Exp. Med., 2024 August, **263** (4), 249-259.
doi: 10.1620/tjem.2024.J030

Introduction

Among the deaths caused by cardiovascular diseases, myocardial cell apoptosis resulting from ischemia is an established cause of mortality in individuals. Hence, cardiomyopathy induced by ischemia has become a significant threat leading to disability or death in developing nations (Zhou et al. 2018). Acute myocardial infarction during the early stages, coupled with impaired myocardium, imbalances the electric activity and ventricular polarization, resulting in arrhythmia and eventually death (Oknińska et al. 2022). An efficient strategy for correcting myocardial ischemia (MI) is retrieving coronary blood flow. However, reperfusion followed by ischemia may worsen cardiac functionality or result in cardiomyocyte damage, leading to increased intracellular calcium burden, inflammation, and finally, apoptosis (Neri et al. 2017). Exploring this functional scheme is crucial for effectively implementing strategies for managing MI and reperfusion damage.

The cellular overburden of calcium is the most substantial factor that induces cardiac arrhythmia. Sodium-potassium ATPases (Na^+-K^+ATPase) and calcium-magnesium ATPases (Ca^{2+}-Mg^{2+}ATPase) are crucially involved in balancing the cellular calcium feedback mechanism, but in individuals with cardiac arrhythmia, the functionality of these enzymes in tissues of the myocardium is lowered (Kistamás et al. 2020). The inter-cardiomyocyte intersection spacing is the morphological basis for the dissipation

Received March 14, 2024; revised and accepted May 16, 2024; J-STAGE Advance online publication May 24, 2024
*These two authors contributed equally to this work.
Correspondence: Qi Wu, Department of Cardiovascular Medicine, The Second Affiliated Hospital of Chengdu Medical College, China National Nuclear Corporation 416 Hospital, Chengdu, Sichuan 610057, China.
e-mail: wuqi37157@163.com

of action potential associated with myocardial tissues and is critically involved in the electric signal and its threshold transmission, which eventually relies on the alteration of gap junction connexin (Dhein and Salameh 2021). Twenty-one members of the connexin family, with a molecular weight ranging from 26 to 60 kDa, are present in different organs and cells (Garcia-Vega et al. 2021). Ventricular cardiomyocytes have an abundant presence of the Gap Junction alpha-1 (GJ*α*-1) protein, commonly referred to as connexin 43, with lesser expression in endothelial cells, fibroblasts, and atrial cardiomyocytes (Pun et al. 2023). GJ*α*-1 is required for signal transmission among the myocardial cells. Expression and allocation of GJ*α*-1 are crucial for balancing electrical signals and activity in the cardiac gap channels, thereby harmonising cardiac muscles' contraction (Leybaert et al. 2023). Reports reveal that normal distribution and activity of GJ*α*-1 are critically required for maintaining the standard myocardial functionality of the heart (Grune et al. 2021).

Gastrodin (GD) is a phenolic glycoside obtained from the dried roots of *Gastrodia elata f. glauca*. Fig.1 shows the chemical structure of the GD. It is often used in traditional Chinese medicine and has a low level of toxicity. GD is frequently used in the treatment of vascular and neurological disorders. Recently, several studies have shown that gastrodin has anti-osteoporosis properties. Its modes of action include antioxidant, anti-inflammatory, and anti-apoptotic actions. (Long et al. 2020). GD can reduce intracellular Ca^{2+} load and can act as a calcium channel blocker (Park et al. 2023). Increased arterial flexibility, increased blood supply, and lowered blood viscosity, thereby improving microcirculation, could be observed with GD treatment (Sutresno et al. 2020). GD induces a marked reduction in lipid peroxidation levels, substantiates free radical scavenging activity, inhibits oxidative phosphorylation, and enhances the activity of genes that encode antioxidant protein production (Chaudhary et al. 2023). The findings of a study on cardiac hypertrophy in mice demonstrated that the inhibitory effects of GD are facilitated through ERK1/2 signalling and the stimulation of GATA-4 (Pang et al. 2021). In the present investigation, a rat model of myocardial I/R was developed and studied to determine the effect of GD treatment on the expression of GJ*α*-1 coupled with normal ventricular harmony; also, the molecular mechanism involved in correcting cardiac arrythmia by GD treatment was investigated.

Material and Methods

Experimental animals and treatment groups

In this investigation, 40 male healthy Sprague Dawley rats (300-350; 80-90 days) were procured from the animal facility of The second affiliated Hospital of Chengdu Medical College, Sichuan, China, and were accommodated in clean and hygienic conditions. The investigations adhered to the procedure outlined in the National Institutes of Health Guide for the Care and Use of Laboratory Animals (USA), as well as the ethical guidelines set by the second affiliated hospital of Chengdu Medical College (Reg. No. 483626/2022/MY/CN/2948). The study also followed the recommended guidelines for animal maintenance and practice. The animals were allowed full access to food as well as water in vented rooms kept at 20-25°C and 55-60% moisture content with a 12:12 light-dark pattern. Gastrodin (GD) (CAS *62499-27-8)* (purity > 98%) was purchased from Chengdu Herbpurify Co., Ltd., Chengdu, China.

The experimental subjects were randomly allotted into any one of the four groups (n = 10), the Sham group, the model group, the GD 50 group (pre-treated with 50 mg/kg; 1 ml for each rat), and the GD 100 group (pre-treated with 100 mg/kg; 1 ml into ip. for each rat). The GD was injected intraperitoneally (i.p.) 10 mins before induction of ischemia in rats from the GD 50 and GD 100 groups. On the other hand, the two remaining groups of animals, namely the Sham group and the model group, received an equivalent amount of sterile saline solution via injection.

Animal model of I/R injury

The myocardial I/R animal model was established according to the methodology reported by Zhou et al. (2023). Initially, the rats were exposed to anaesthesia intraperitoneally (5% Urethane) and were laid flat on their backs over an operating table. ECG recordings for normal cardiac functions were obtained noninvasively using the ECGenie apparatus (Mouse Specifics, Inc., Framingham, MA) as previously described by Monroe et al. (2016). The rats that did not indicate normal cardiac cycles were eliminated from the investigation. A respiration measuring machine (Yonker YK-8000a, Xuzhou ETDZ, Xuzhou, China) for animals, having an 8 ml/kg tidal volume, a frequency of respiration of 70/minute, and a breathing in and out ratio of 2:1, respectively, was cannulized into the bronchi. In the left carotid artery, a tube was penetrated for epidural anaesthesia. The electrophysiological signals were also recorded from the same carotid artery. To induce ischemia in the rats from the model and experimental groups, the descending end of the left coronary artery was blocked by ligation using 4/0 silk sutures, whereas no ligation was done in the rats from the Sham group. The ischemia was induced for 30 mins, after which the animals were subjected to reperfusion for 2 hours, and the ECG pattern was recorded. An elongated ST section or increased extent of the QRS wave, coupled with a broader wave and merger of the T-wave, a drop in arterial pressure of 20 mm Hg, and the appearance of peripheral cyanosis in the vicinity of the ligation, confirmed the development of the ischemia model. The success of the reperfusion model was confirmed by the fading of cyanosis, a more than half reduction in the elevation of the ST segment after 30 mins of reperfusion, the absence of atrioventricular blockage before surgery, and a reduction of mean artery pressure below 60 mm Hg. HR, MAP, and RPP were recorded in animals at 10 mins (T0) before ischemia, 30 mins following ischemia

(T1), 30 mins (T2), 60 mins (T3), and 120 mins (T4) following reperfusion, together with monitoring cardiac arrhythmia in experimental rats.

Arrhythmia score

The arrhythmia score was evaluated using the minor modification approach previously described by Yang et al. (2018). The Lambeth Conventions were used to carefully examine the arrhythmias, and the severity of the arrhythmias was determined according to the standards established by Walker and Curtis.

Hematoxylin-eosin (HE) staining

In this study, histopathological studies were performed based on the improved method of Zhang et al. (2017). After 2 hrs after reperfusion, the heart was quickly removed from the individual animal, rinsed, and fixed in 4% paraformaldehyde. After 24 hrs, the specimens were dehydrated with the help of ethanol, incorporated into a paraffin block, and sliced using an ultramicrotome (EM UC7 Ultramicrotome, Leica Microsystem, Guangdong, China). The resulting slices (5 μm) were stained using HE and visualized using a light-field microscope (× 400 magnification).

Assessment of Na^+-K^+ATPase and Ca^{2+}-Mg^{2+}ATPase levels

The experiment assessed the levels of Na^+-K^+ATPase and Ca^{2+}-Mg^{2+}ATPase using the modified approach developed by Ji et al. (2009). The myocardial tissues below the ligature were separated, added to the normal saline solution at a weight ratio of 1:9, and subjected to homogenization in the cold. The homogenate underwent centrifugation at 800 *g* for 10 mins. The supernatant was collected and employed to assess the levels of Na^+-K^+ATPase and Ca^{2+}-Mg^{2+}ATPase expression. This was accomplished by utilizing kits from the Jiancheng Biological Engineering Institute in Nanjing, China.

Assessment of CK-MB, cTnI and LDH

The study evaluated the concentrations of CK-MB, cTnI, and LDH using the modified technique developed by Ren et al. (2021). The specimens of blood were obtained following 2 hrs of reperfusion and subsequently underwent centrifugation at 1,200 *g* for 15 mins. The supernatant was separated and analyzed for the estimation of creatinine kinase myocardial band (CK-MB), cardiac troponin I (cTnI), and lactate dehydrogenase (LDH) levels. A microplate analyzer was used to determine the absorbance at 450 nm.

Assessment of the anti-oxidative potential of GD

The antioxidant capacity of GD was evaluated using the modified approach described by Farhangi et al. (2017). The cardiac tissues were collected and subjected to homogenization by Enrichment Sample Homogenizer (ESH) by Mark, Merck Ltd., Chengdu, China) using phosphate-buffered saline (PBS) and centrifuged at 10,000 *g* at 4°C for 20 mins. The supernatant was gathered and analyzed for the determination of malondialdehyde (MDA) by Ben Attig et al. (2023) and superoxide dismutase (SOD) by Soto et al. (2014). using commercially available test kits (Jiancheng Biological Engineering Institute, Nanjing, China), following the instructions supplied by the manufacturer.

Assessment of immunochemical markers expression

The experimental animals were sacrificed with a bolus dose of anaesthesia, and the hearts were separated. The ventricles were isolated from the heart and subjected to cryopreservation in liquid nitrogen (–80°C) until further investigation. The myocardial protein was extracted using a blend of protease inhibitors (Roche Applied Science, USA) and CelLytic MT tissue lysis and extraction reagents (Sigma Aldrich, USA). The tissue mass was crushed in a homogenizer (BeadBug™ microtube homogenizer, Sigma-Aldrich®, China) for 30 mins at 4°C, and then cryo-centrifuged for 15 mins at 3,000 *g*. The protein content was measured by sodium dodecyl sulphate polyacrylamide gel electrophoresis (SDS-PAGE) and then moved onto a polyvinylidene difluoride membrane (Millipore, USA) in buffer containing 20 mmol/L Tris hydrochloride, 0.15 mol/L glycine, and 20% methanol, employing the Trans-Blot system (Bio-Rad Laboratories, USA). The membranes were obstructed using skimmed milk and exposed to a tris buffer saline solution with tween 20 surfactant (Sigma Aldrich, USA) for an hr at 25ºC. Further, the membranes were treated for 12 hrs at 25°C with antibodies against Kir2.1 (Boster Bio, China), GJα-1 (#3512), phosphorylated-GJα-1 at Ser368 (#3511), Bax (#2774), Bcl-2 (#15071), GAPDH (#97166), and β-actin (#3700) (Cell Signalling, Shanghai, China). Following that, the membranes were exposed to incubation with a secondary antibody coupled with horseradish peroxidase (HRP) for an hour. The intensity of the developed immunoblots was detected using Gel Pro Software (Media Cybernetics, MD, USA). To normalize the protein levels, β-actin and GAPDH were used as normalization controls.

Characterization of In silico molecular docking

A *silico* molecular docking evaluation was conducted to investigate the potential binding interaction between the selected molecule GD and the protein GJα-1, which has been identified *in vivo*. For the docking study, the ligand GD and protein GJα-1 were prepared before analysis. The protein crystal framework of GJα-1 was collected from the protein database as a pdb extension file, whereas the structure of ligand GD was prepared using ChemDraw. Both structures were formatted and prepared by removing any water molecules, minimizing energy, and adding Kolmann charges. Both structures were prepared and converted in.pdbqt files as required for AutodockVina MGL tools for docking. For initiating the docking, the grid box was prepared with dimensions of x = –2.541, y = 9.121, and z = 18.144, the coordinate size was selected to be 20, the exhaustiveness was 8, and energy was 4. The docking oper-

ation was run using Autodock Vina MGL tools. The figures and output files were viewed using the software Pymol, which showed the interactions of ligands and proteins.

Statistical assessment

The data was statistically assessed using licensed SPSS (Version 19.0, Chicago, USA). The data is characterized as the mean ± SD. The ratios were compared using Chi-square analysis. The ratio phospho-Cx43/Cx43 was processed by one-way ANOVA and subsequently by the Bonferroni test among the two groups. The statistical threshold was kept at $p < 0.05$.

Results

GD modulates hemodynamic and arrythmia

Animals from the model group and experimental groups GD50 and GD100 showed lower HR, MAP, and RPP than the Sham group animals at T1, T2, T3, and T4. Model group animals exhibited significantly ($p < 0.05$) lower HR, MAP, and RPP at T1, T2, T3, and T4 than Sham group animals. However, animals from the GD50 and GD100 groups had higher values of HR, MAP, and RPP than model group animals ($p < 0.05$) at T1, T2, T3, and T4. Also, there was a marked ($p < 0.05$) difference between the HR, MAP, and RPP between the GD50 and GD100 groups. (Fig. 1A-C). The model group (4.56), the GD50 group, and the GD100 group all had significantly ($p < 0.05$) higher cardiac arrhythmia scores (3.22 and 1.72) than the Sham group (1.17), as shown in Fig. 1D.

GD attenuates myocardial damage

Animals from the Sham group exhibited the usual myocardial architecture and uniform distribution of the myocardial filaments. Inflammatory cell infiltration in the mesenchymal myocardium and the non-uniform arrangement of myocardial filaments were depicted in the morphology of myocardial tissues from model group animals that were subjected to myocardial I/R injury in comparison to specimens collected from sham group animals. However, the myocardial damage was less pronounced in myocardial tissues retrieved from animals that were pre-treated with GD in comparison to that from the model group. Myocardial tissue fractions collected from GD100 group animals showed a marked reduction in myocardial damage compared to that visualized in model and GD50 group animals (Fig. 2).

GD enhances Na^+-K^+ATPase and Ca^{2+}-Mg^{2+}ATPase expression

The administration of GD resulted in an increase in the levels of Na^+-K^+ATPase and Ca^{2+}-Mg^{2+}ATPase expression in the myocardial tissues of rats, as depicted in Fig. 3A, B. Rats from the model group and GD50 and GD100-treated groups had relatively reduced ($p < 0.05$) activity of Na^+-K^+ATPase and Ca^{2+}-Mg^{2+}ATPase compared to the Sham group rats. However, the activity of Na^+-K^+ATPase and Ca^{2+}-Mg^{2+}ATPase was substantially higher ($p < 0.05$) in the GD50 (26.08 & 27.96) and GD100 (27.81 & 29.55) treated groups in comparison to those from the model group (24.89 & 25.68) that were left untreated with GD. Among the GD50 and GD100 pre-treated animal groups, there was a

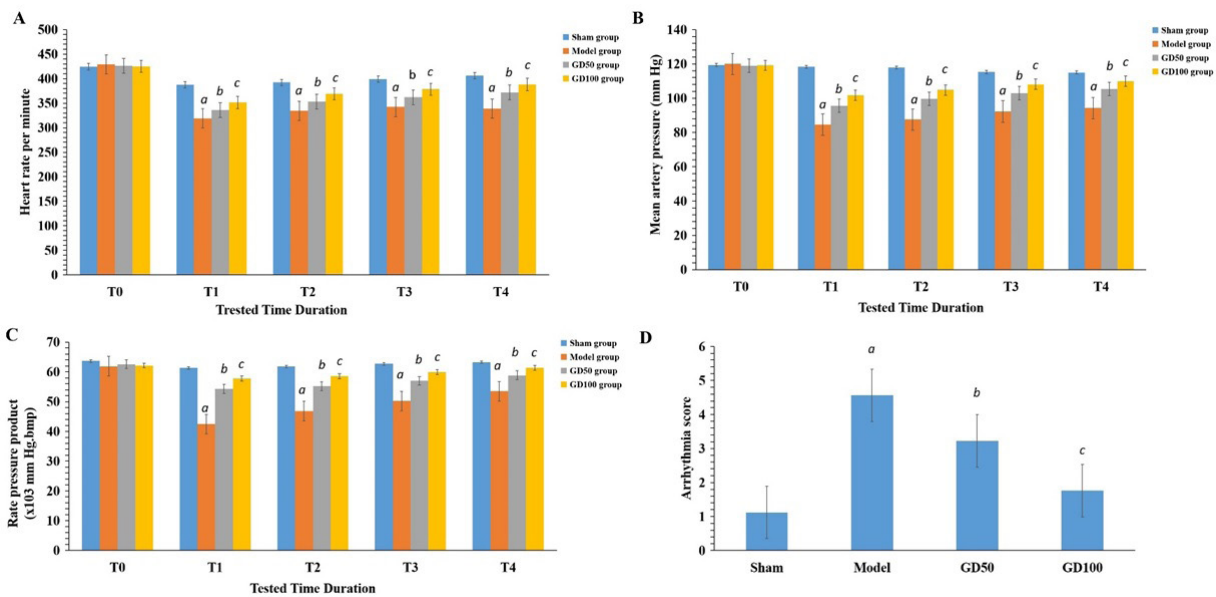

Fig. 1. Effect of Gastrodin pre-treatment on (A) heart rate, (B) mean arterial pressure, (C) rate pressure product and (D) arrhythmia score in myocardial I/R rat model.
T0: 10 mins before ischemia; T1: 30 mins after ischemia; T2: 30 mins after reperfusion; T3: 60 mins after reperfusion; T4: 120 mins after reperfusion. *a*: $p < 0.05$ compared to the Sham group; *b*: $p < 0.05$ compared to the Model group, *c*: $p < 0.05$ compared to the GD50 group.

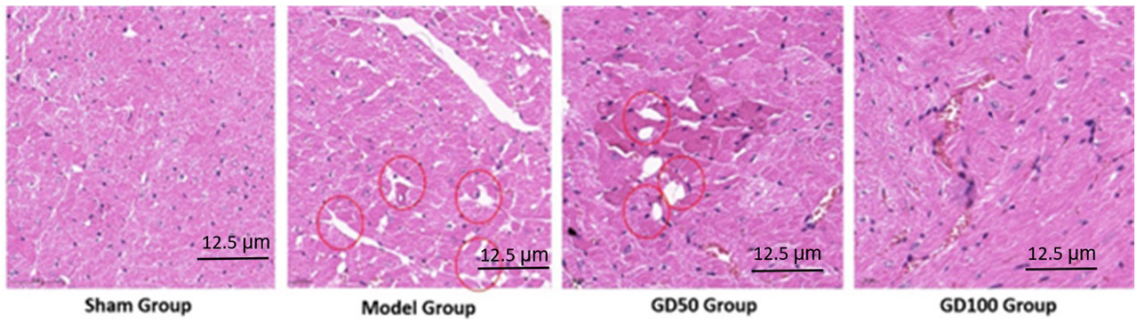

Fig. 2. Effect of Gastrodin pre-treatment on myocardial tissue morphology in experimental groups animals visualized after HE staining (× 400 magnification).
A. Sham group, B. Model group, C. GD50 group, and D. GD100 group.

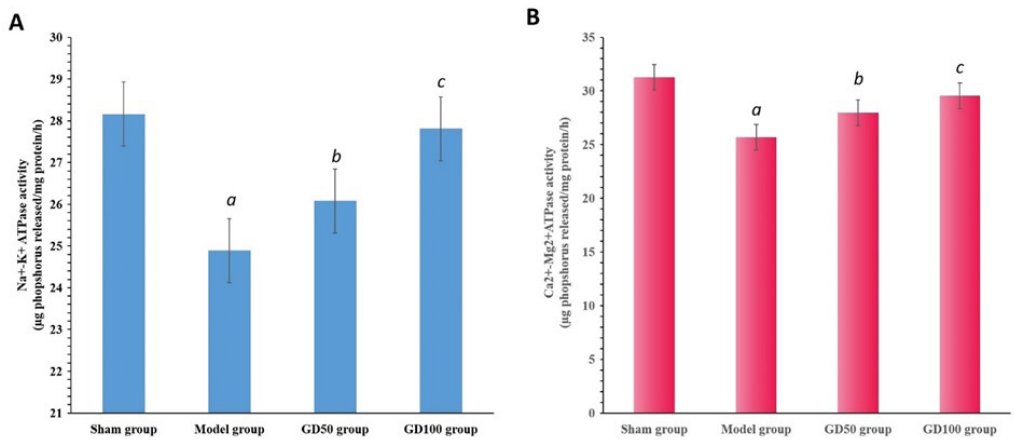

Fig. 3. Effect of Gastrodin pre-treatment on Na^+-K^+ATPase and Ca^{2+}-Mg^{2+}ATPase levels in myocardial I/R rats.
a: $p < 0.05$ compared to the Sham group; *b*: $p < 0.05$ compared to the Sham group, *c*: $p < 0.05$ compared to the Sham group.

substantial variation ($p < 0.05$) within the action of Na^+-K^+ATPase and Ca^{2+}-Mg^{2+}ATPase.

GD effectively reduces the CK-MB, cTnI, and LDH levels

In comparison to the Sham group animals, the animals from the model group (109.63 U/L and 5.36 mg/mL) and the GD50 (72.82 U/L and 3.26 mg/mL) and GD100 (45.88 U/L and 3.09 mg/mL) pre-treated groups had substantially greater ($p < 0.05$) expression of CK-MB and cTnI (Fig. 4A, B). The animals belonging to the GD100 groups exhibited substantial variation ($p < 0.05$) compared to both the model group and the GD50 group animals. Similar behaviour was seen with LDH levels among the experimental groups. The animals belonging to both the model group (2,109 U/L) and the GD-treated groups (1,883 U/L and 1,659 U/L) exhibited considerably higher levels ($p < 0.05$) of LDH in comparison to the animals in the Sham group (1,513 U/L) (Fig. 4C). Although there was a marked difference in the LDH levels between the GD50 and GD100 groups and between the model and the GD100 group, In general, the animals in the GD100 and GD50 groups exhibited considerably reduced expression of CK-MB and cTnI, as well as a lower level of LDH, compared to the model group ($p < 0.05$). The findings of this study suggest that the levels of CK-MB and cTnI expression, along with the LDH level, were normalized to levels similar to those observed in the Sham group animals.

GD lowers the oxidative stress

Lipid peroxidation occurring during I/R injury indicates oxidative stress, which is estimated by determining the MDA level. Also, a reduction in the SOD level indicates oxidative damage caused by I/R injury. The results of this study demonstrated a substantial rise ($p < 0.05$) in the levels of MDA in the model group (8.06 nmol/mg) compared to the GD50, GD100, and sham groups (7.11 nmol/mg, 6.18 nmol/mg, and 5.86 nmol/mg) (Fig. 5A). The levels of SOD were considerably decreased ($p < 0.05$) in the model group (39.68 U/mg) compared to the other tested GD50 (59.63 U/mg), GD100 (72.87 U/mg), and sham groups (77.59 U/mg) (Fig. 5B). The findings of this study, in animals subjected to I/R injury and pre-treated with GD 50 mg/kg and 100 mg/kg, indicated a remarkable ($p < 0.05$) reduction in the MDA levels and considerable elevation ($p < 0.05$) in the level of SOD, advocating an antioxidant effect induced by GD. Comparisons within experimental groups GD50 and GD100 indicated that there was a signifi-

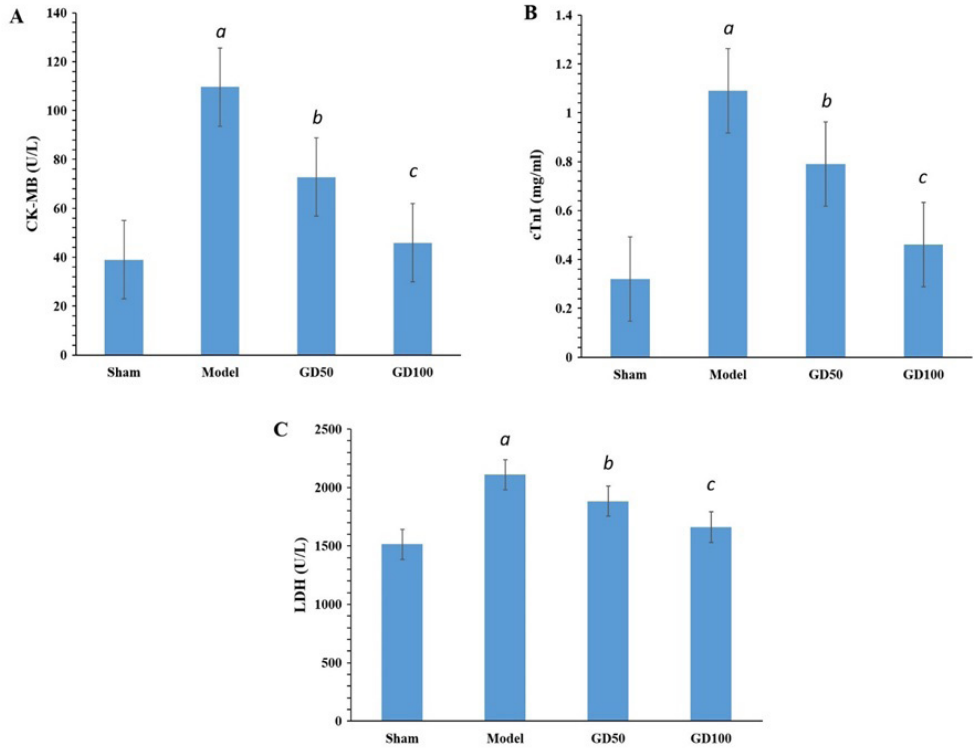

Fig. 4. Effect of Gastrodin pre-treatment on (A) CK-MB expression, (B) cTnI expression, and (C) LDH level in myocardial I/R rats.
a: $p < 0.05$ compared to the Sham group; *b*: $p < 0.05$ compared to the Model group, *c*: $p < 0.05$ compared to the Sham group.

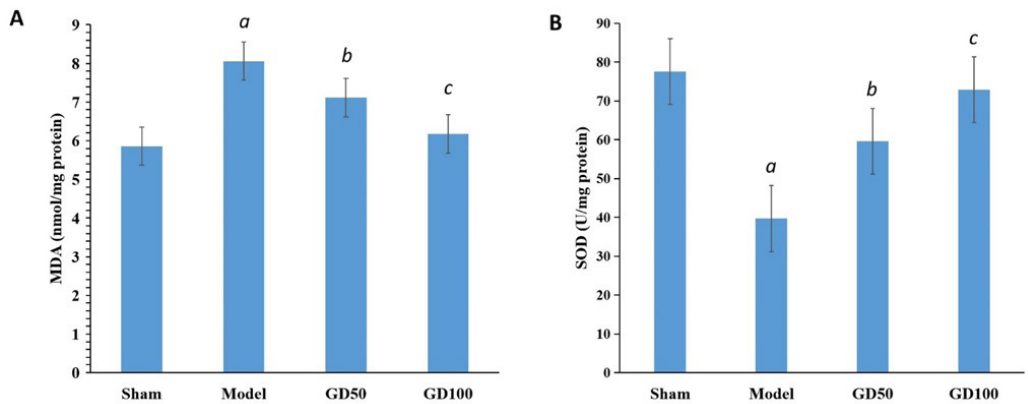

Fig. 5. Effect of Gastrodin pre-treatment on (A) MDA, and (B) SOD level in myocardial I/R rats.
a: $p < 0.05$ compared to the Sham group; *b*: $p < 0.05$ compared to the Model group, *c*: $p < 0.05$ compared to the Sham group.

cant effect observed in the modulation of oxidative stress markers in GD100 group animals.

GD modulated the expression of immunochemical markers

Administration of GD remarkably ($p < 0.05$) elevated the phospho-GJα-1/total-GJα-1 ratio, which indicates ischemic myocardium relative to the non-ischemic myocardium ratio, in comparison to I/R model rats that were untreated with GD (Fig. 6A, C). Expression of protein Kir2.1 was lower in animals from the model group and GD-treated group relative to animals from the Sham group (Fig. 6A, B). GD-treated animals had significantly ($p < 0.05$) higher Kir2.1 protein expression (0.61 and 0.83) compared to the animals from the model group (0.43). GD-treated animals had significantly ($p < 0.05$) higher Kir2.1 protein expression (0.61 and 0.83) compared to the animals from the model group (0.43). The Sham group had high levels of both total GJa-α1 and phospho-GJa-α1 protein expression. However, the expression levels were lower in the model group (0.23 and 0.14) and the tested GD groups (GD50

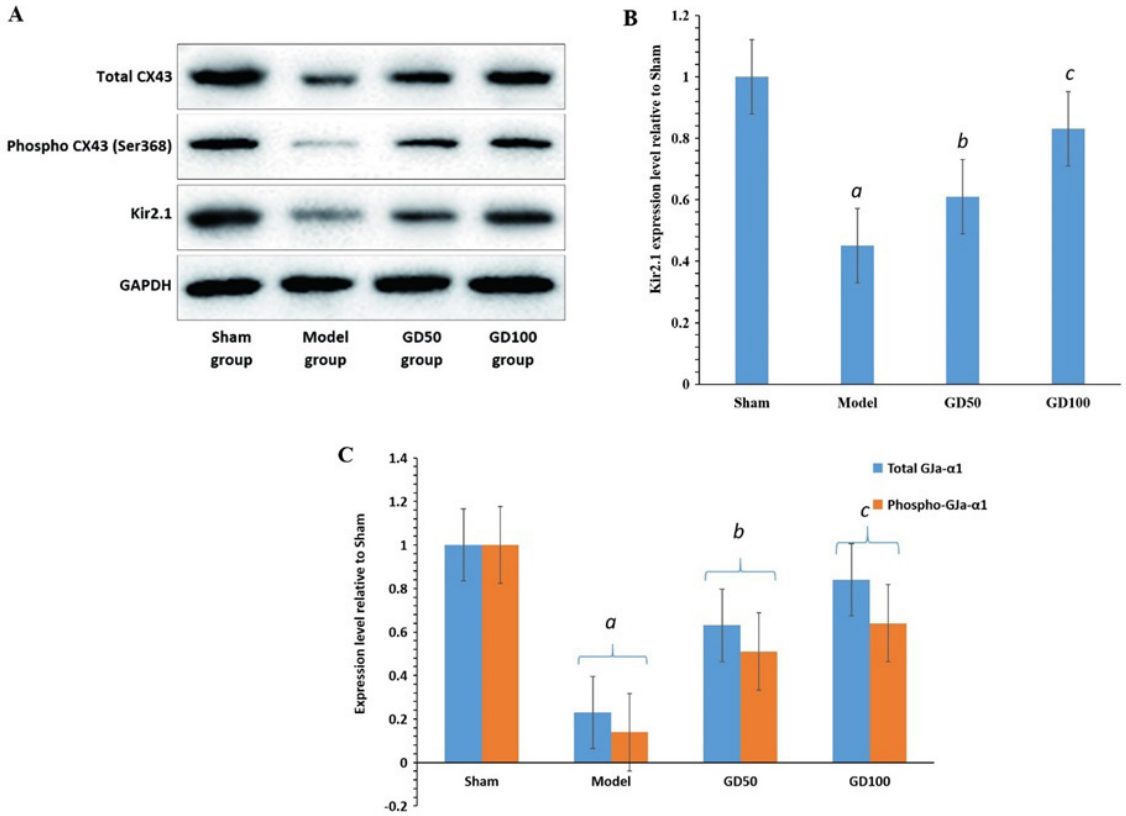

Fig. 6. Effect of Gastrodin pre-treatment on phospho-GJα-1, total GJα-1 and Kir2.1 protein expression in myocardial I/R rats.
(A) representative Western blots and (B) corresponding graphical representation. *a*: $p < 0.05$ compared to the Sham group; *b*: $p < 0.05$ compared to the Model group, *c*: $p < 0.05$ compared to the Sham group.

(0.63 and 0.51) and GD 100 (0.84 and 0.64) (Fig. 6C).

The animals in both the model group and experimental group exhibited significant upregulation of Bax and down-regulation of Bcl-2 in comparison to the animals in the Sham group ($p < 0.05$). However, in animals from the GD-treated group, this expression was slightly close to that observed in Sham group animals, compared to model group animals. There was a considerable difference in the Bax and Bcl-2 expression within the model group (0.69 & 0.26) and GD50 (0.42 & 0.48) and GD100 animals (0.35 & 0.89) ($p < 0.05$) (Fig. 7A, B).

GJα-1 had a higher binding affinity for GD.

The results of molecular docking analysis suggested that GD had a higher binding affinity for GJ*α*-1. The values of lower binding energies suggested that the ligand GD, upon interacting with protein GJ*α*-1, resulted in low energy scores (Table 1). The 3D structure of protein GJ*α*-1 with GD showed potential binding of the ligand to the protein (Fig. 8A, B).

Discussion

Myocardial I/R injury results from several clinical aspects, such as coronary bypass surgery, cardio-pulmonary resuscitation, thrombolytic risk, and heart replacement. Associated attributes of myocardial I/R include post-ischemic arrythmia, myocardial stress, cardiomyocyte destruction, and no chances of reflow. These disturbances may result in critical impairment and the death of the individual (He et al. 2022). Therefore, there is an obligatory need to explore novel molecules to address the myocardial I/R injury issue efficiently.

GD is a therapeutic molecule that has been identified as exerting several pharmacological impacts on cardiovascular and cerebrovascular disorders. However, there has been limited knowledge about the protective influence of GD on myocardial I/R injury and arrythmia in a rat model and its possible mechanism. Hence, the investigation was envisaged to explore the effect and mechanism of GD in the reduction of MI-reperfusion injury and cardiac arrhythmia in rats. It is widely known that ventricular arrhythmia-related deaths may occur as an outcome of myocardial I/R damage (Singhanat et al. 2020). Hence, arrythmia scores in all experimental animals were determined in the present investigation. The animals that underwent myocardial ischemia/reperfusion (I/R) injury exhibited a significantly higher arrhythmia score compared to the animals in the Sham group. However, GD administration before surgical intervention ameliorated myocardial I/R injury and reduced the arrythmia score in experimental rats in comparison to

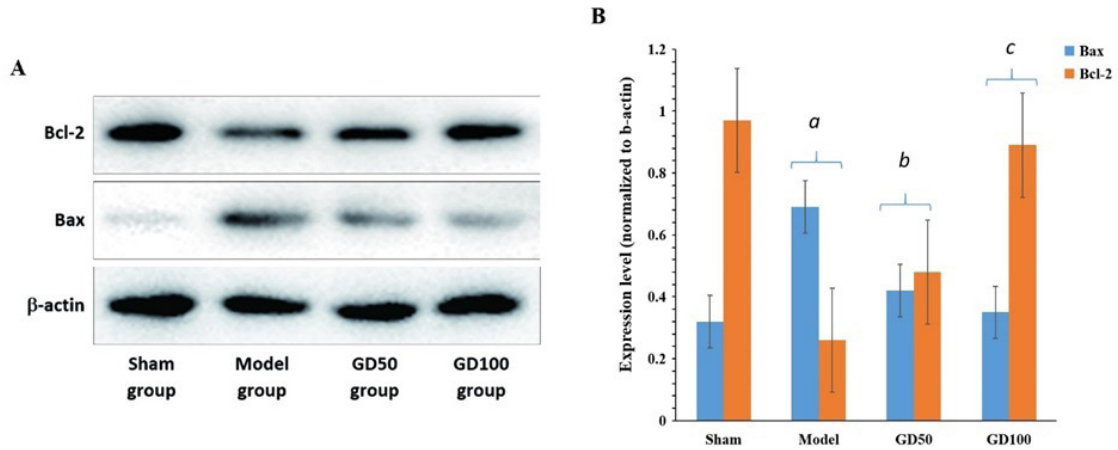

Fig. 7. Effect of Gastrodin pre-treatment on Bax and Bcl-2 protein expression in myocardial I/R rats. (A) representative Western blots and (B) corresponding graphical representation. *a*: $p < 0.05$ compared to the Sham group; *b*: $p < 0.05$ compared to the Model group, *c*: $p < 0.05$ compared to the Sham group.

Table 1. Docking scores for protein GJα-1 with the ligand GD.

Mode of ligand	Affinity (kcal/mol)	Distance from rmsd l.b	Best mode rmsd u.b
1	–8.2	0.000	0.000
2	–8.2	19.225	18.241
3	–8.0	3.215	8.220
4	–7.9	6.511	7.160
5	–7.8	17.210	20.122
6	–6.8	4.215	6.121
7	–6.6	20.227	21.421
8	–6.5	20.120	21.546
9	–6.5	2.291	5.220

those in the model group.

In our investigation, a 30-mins myocardial ischemic event followed by a 2-hour reperfusion episode of the left coronary artery resulted in substantial impairment of HR, MAP, and RPP in rats, coupled with a marked enhancement in the arrhythmic score. These findings confirmed the successful development of a myocardial I/R injury in experimental rats. In rats from the Sham group, there were no statistically substantial variations in the HR, MAP, or RPP. Rats subjected to myocardial I/R damaged suffer severe reductions in HR, MAP, and RPP. However, treatment of myocardial I/R damage animals with GD revealed significant improvisation in the HR, MAP, and RPP values. A substantial reduction in the arrhythmic score and normalisation of the HR, MAP, and RPP indicate the protective impact of GD in rats with myocardial I/R injury.

Several factors are concerned with the development of heart disorders and their progression. Cardiomyocytes may undergo deterioration and mortification after an ischemic episode. Injury mediated by reperfusion may enhance the membrane penetrability of cardiomyocytes and the serum expression of markers associated with injury to myocardial tissues (Nasiłowska-Barud et al. 2017). Cell membrane damage results in increased LDH leakage and is hence regarded as an important biomarker of myocardial damage during reperfusion (Wang et al. 2019). The present investigation exhibited marked elevation in the LDH in the rats exposed to myocardial I/R injury, whereas in rats that were given GD, there was a marked reduction in the LDH level. These findings advocate that GD may partially occur through this mechanism, resulting in attenuation of the myocardial injury due to I/R. Also, the magnitude of the myocardial tissue damage is associated with the levels of CK-MB and cTnI (Promsan et al. 2016). CK-MB is a highly sensitive detector for MI, whereas cTnI, a specific protein present in myocardial tissues, is almost untraceable in the serum under normal cardiac conditions, but its release is initiated in the circulation if the myocardial cell membrane no longer remains intact. In general, elevated levels of CK-MB and cTnI in an individual are an indication of myocardial muscle damage (Wu et al. 2021). Hence, the obvious biomarkers used to diagnose and detect damage to the myocardial tissues due to ischemia are CK-MB and cTnI. In our investigation, the CK-MB and cTnI levels were considerably greater in the myocardial tissues that were subjected to myocardial I/R injury compared to the

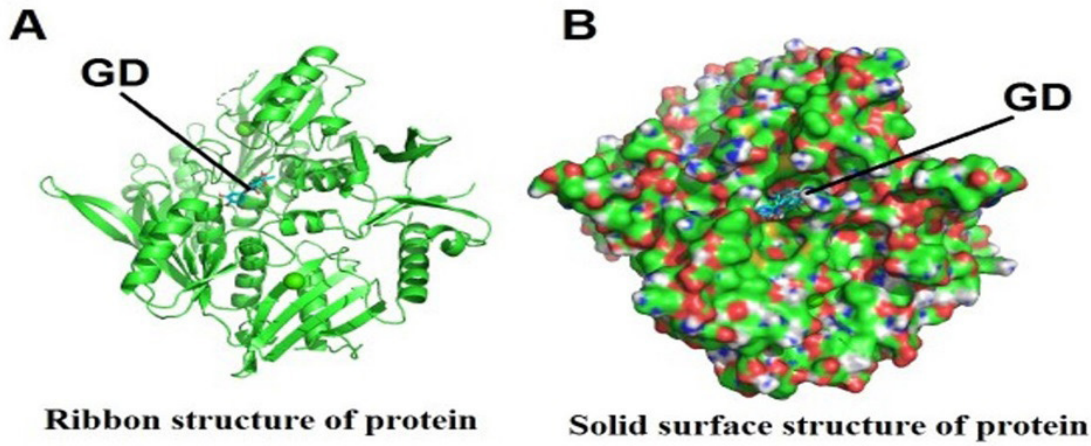

Fig. 8. Effect of Gastrodin pre-treatment on binding affinity for GJα-1.
Ribbon structure and (B) Solid surface structure of interaction between GJ*α*-1 protein and GD.

Sham group. However, GD treatment revealed a marked reduction in the CK-MB and cTnI levels in the serum of rats with myocardial I/R injury. The findings provide convincing evidence that GD could attenuate the injury in myocardial tissues caused by ischemia and reperfusion.

Oxidative phosphorylation in the mitochondria and the production of ATP are markedly reduced after an increase in Ca^{2+} in the mitochondrial matrix due to MI (Boyman et al. 2020). After an ischemic event, there is a notable surge in reactive oxygen species and associated oxidative stress markers that further lead to damage to the cell membrane, thereby enhancing cell permeability. In the present investigation, the levels of MDA and SOD were measured. After a severe oxidative stress challenge, as in MI, the MDA levels are known to increase, indicating lipid peroxidation, whereas the level of an antioxidase, SOD, is found to be reduced (Hong et al. 2017). Results from our investigation revealed increased levels of MDA in the myocardial tissues collected from rats that were exposed to myocardial I/R injury, whereas the levels were lowered in rats that were treated with GD. In animals from the ischemic model group, the myocardial tissue SOD level was lowered, and the level was enhanced in the myocardial tissues of rats in the GD-treated group. The neuroprotective activity of GD against cerebral ischemia is due to its anti-inflammatory and antioxidant effects (Emmez et al. 2022).

Overload of Ca^{2+} is an important mediator in the induction of myocardial I/R injury (Wang et al. 2018). Na^{+}-K^{+}ATPase is a membrane protein and is required for the conversion of cell energy. Ischemia resulting in cardiac dysfunction inhibits the activity of Na^{+}-K^{+}ATPase at the level of the sarcolemma, thereby leading to the accumulation of extracellular K^{+} and intracellular Na^{+} (Obradovic et al. 2023). Significant cardiac damage during myocardial I/R injury is reflected by lowered Na^{+}-K^{+}ATPase. Ca^{2+}-Mg^{2+}ATPase is triggered due to increased Ca^{2+} to an extent when Ca^{2+} is moved out of the cells, thereby reducing intracellular Ca^{2+} concentration. Reports suggest that Ca^{2+}-Mg^{2+}ATPase activity is markedly reduced in the event of myocardial I/R injury (Xie et al. 2016). The results of our investigations revealed that the expression of both Na^{+}-K^{+}ATPase and Ca^{2+}-Mg^{2+}ATPase is reduced in the myocardial tissues of rats subjected to myocardial I/R injury. Pretreatment with GD revealed a marked increase in the activity of Na^{+}-K^{+}ATPase and Ca^{2+}-Mg^{2+}ATPase in the myocardial tissues that experienced myocardial I/R injury. The findings advocate the cardioprotective effect of GD, as revealed by balancing the energy metabolism and overloading Ca^{2+}.

Myocardial cell apoptosis is triggered after the reperfusion injury, which further progresses to severe damage to the cardiac tissues (Belliard et al. 2016; Wang et al. 2020; Lodrini and Goumans 2021). During the apoptotic process, Bax and Bcl-2 proteins play a significant role in regulating the permeability of the exterior mitochondrial membrane (Qian et al. 2022). Bax stimulates the formation of pores, and Bcl-2 impedes the same. Bax modulates mitochondrial functionality and activates the caspase cascade, which further aggravates the apoptotic process (McKenna et al. 2021). Overall, Bax and Bcl-2 are employed as critical markers of apoptosis. Results from our investigation exhibited that GD reduced the elevated Bax expression, which is a pro-apoptotic protein, after an event of myocardial I/R injury without influencing Bcl-2 expression, which is an anti-apoptotic protein. The intactness of mitochondria could be expected to be favoured as the Bax/Bcl-2 ratio significantly displaces Bcl-2 (Qian et al. 2022). These findings provide evidence that GD triggers an anti-apoptotic effect in myocardial I/R injuries.

Out of several gap junction connexins present in the body, GJ*α*-1 is of critical significance in sustaining the regular performance of the myocardial tissues. The GJ*α*-1 protein, encoded by the GJA1 gene, is disseminated in cardiomyocyte junctions to execute the transmission of cellular and biochemical information and energy transfer. GJ*α*-1 is responsible for harmonising the cardiac cycle and maintain-

ing the electrical activity of the heart (Kajiwara et al. 2018). One more protein that is of utmost importance in maintaining the consistency of the resting potential of the membrane is Kir2.1, encoded by the gene KCNJ2. Dephosphorylation of GJ*α*-1 could lead to a lowering of cellular energy and extend the span of action potential and repolarization, thereby resulting in transmission blockage. Disturbances in the availability and expression of GJ*α*-1, lead to discontinuity of the intracellular electrical transmission and cause arrythmia (Chang et al. 2015). A reduction in the expression or function of Kir2.1 induces repolarization during phase 3 of the action potential, thereby extending it and leading to cardiac arrythmia (Reilly and Eckhardt 2021). During an event of myocardial I/R injury, the GJ*α*-1 dephosphorylation results in an attenuation of communication between gap junctions within the myocardial cells, ultimately leading to cardiac arrythmia (Peng et al. 2022). A reduction in the phosphorylation of GJ*α*-1 during myocardial I/R injury leads to an increase in the arrythmia score (Yang et al. 2021). The findings of our investigation revealed a significant rise in the phospho-GJ*α*-1/total-GJ*α*-1 ratio and Kir2.1 in the myocardial fractions of GD-treated rats compared to those left untreated, thereby testifying to the reduction in arrythmia score. Also, the results of molecular docking suggested potential binding between GD and GJ*α*-1. Phosphorylation of GJ*α*-1 at Ser368 blocks phosphorylation of GJ*α*-1 at its other residues, which modulates the transmissions in cellular gap junctions, thereby inhibiting cardiac arrythmia (Zhang et al. 2023). An increase in the phospho-GJ*α*-1/total-GJ*α*-1 ratio and Kir2.1 expression may both be involved together to disclose the mechanism of GD in attenuating myocardial I/R injury and arrythmia in rats.

Conclusion

In its entirety, the administration of GD treatment exhibited a mitigating effect on arrhythmia in rats that underwent I/R injury. This effect was achieved through the upregulation of Na^{+}-K^{+}ATPase and Ca^{2+}-Mg^{2+}ATPase expression, the targeting of GJ*α*-1, and the modulation of Kir2.1 expression.

Acknowledgements

The authors acknowledge the facilities provided by the superiors.

This study was supported by the Scientific Research Project of Chengdu Science and Technology Bureau (No: 2022-YF05-01459-SN), the Research project of Sichuan Provincial Administration of Traditional Chinese Medicine (No: 2023MS177), Chengdu Key Medical Specialty Project (CDS2022Z076) and Chengdu Key Clinical Specialty Project (CDS2023ZD002).

Author Contributions

The animal studies were conducted by researchers Juan Huang and Guoqu Jia. The docking studies were conducted by Hong Yang. The research inquiry was created and overseen by Qi Wu. The statistical analysis was conducted by Hong Yang. Chunmei Liu and Songjie Bi were responsible for the composition and subsequent revisions of the complete work.

Conflict of Interest

The authors declare no conflict of interest.

References

Belliard, A., Gulati, G.K., Duan, Q., Alves, R., Brewer, S., Madan, N., Sottejeau, Y., Wang, X., Kalisz, J. & Pierre, S.V. (2016) Ischemia/reperfusion-induced alterations of enzymatic and signaling functions of the rat cardiac Na+/K+-ATPase: protection by ouabain preconditioning. *Physiol. Rep.*, **4**, e12991.

Ben Attig, J., Latrous, L., Galvan, I., Zougagh, M. & Rios, A. (2023) Rapid determination of malondialdehyde in serum samples using a porphyrin-functionalized magnetic graphene oxide electrochemical sensor. *Anal. Bioanal. Chem.*, **415**, 2071-2080.

Boyman, L., Karbowski, M. & Lederer, W.J. (2020) Regulation of Mitochondrial ATP Production: Ca(2+) Signaling and Quality Control. *Trends Mol. Med.*, **26**, 21-39.

Chang, Y., Yu, T., Yang, H. & Peng, Z. (2015) Exhaustive exercise-induced cardiac conduction system injury and changes of cTnT and Cx43. *Int. J. Sports Med.*, **36**, 1-8.

Chaudhary, P., Janmeda, P., Docea, A.O., Yeskaliyeva, B., Abdull Razis, A.F., Modu, B., Calina, D. & Sharifi-Rad, J. (2023) Oxidative stress, free radicals and antioxidants: potential crosstalk in the pathophysiology of human diseases. *Front. Chem.*, **11**, 1158198.

Dhein, S. & Salameh, A. (2021) Remodeling of Cardiac Gap Junctional Cell-Cell Coupling. *Cells*, **10**, 2422.

Emmez, G., Bulduk, E.B. & Yildirim, Z. (2022) Neuroprotective effects of adrenomedullin in experimental traumatic brain injury model in rats. *Ulus. Travma Acil Cerrahi Derg.*, **28**, 736-742.

Farhangi, M.A., Nameni, G., Hajiluian, G. & Mesgari-Abbasi, M. (2017) Cardiac tissue oxidative stress and inflammation after vitamin D administrations in high fat- diet induced obese rats. *BMC Cardiovasc. Disord.*, **17**, 161.

Garcia-Vega, L., O'Shaughnessy, E.M., Albuloushi, A. & Martin, P.E. (2021) Connexins and the Epithelial Tissue Barrier: A Focus on Connexin 26. *Biology* (*Basel*), **10**, 59.

Grune, J., Yamazoe, M. & Nahrendorf, M. (2021) Electroimmunology and cardiac arrhythmia. *Nat. Rev. Cardiol.*, **18**, 547-564.

He, J., Liu, D., Zhao, L., Zhou, D., Rong, J., Zhang, L. & Xia, Z. (2022) Myocardial ischemia/reperfusion injury: Mechanisms of injury and implications for management (Review). *Exp. Ther. Med.*, **23**, 430.

Hong, J., Kim, K., Kim, J.H. & Park, Y. (2017) The Role of Endoplasmic Reticulum Stress in Cardiovascular Disease and Exercise. *Int. J. Vasc. Med.*, **2017**, 2049217.

Ji, L., Chauhan, A., Brown, W.T. & Chauhan, V. (2009) Increased activities of Na+/K+-ATPase and Ca2+/Mg2+-ATPase in the frontal cortex and cerebellum of autistic individuals. *Life Sci.*, **85**, 788-793.

Kajiwara, Y., Wang, E., Wang, M., Sin, W.C., Brennand, K.J., Schadt, E., Naus, C.C., Buxbaum, J. & Zhang, B. (2018) GJA1 (connexin43) is a key regulator of Alzheimer's disease pathogenesis. *Acta Neuropathol. Commun.*, **6**, 144.

Kistamás, K., Veress, R., Horvath, B., Banyasz, T., Nanasi, P.P. & Eisner, D.A. (2020) Calcium Handling Defects and Cardiac Arrhythmia Syndromes. *Front. Pharmacol.*, **11**, 72.

Leybaert, L., De Smet, M.A., Lissoni, A., Allewaert, R., Roderick, H.L., Bultynck, G., Delmar, M., Sipido, K.R. & Witschas, K. (2023) Connexin hemichannels as candidate targets for

cardioprotective and anti-arrhythmic treatments. *J. Clin. Invest.*, **133**, e168117.

Lodrini, A.M. & Goumans, M.J. (2021) Cardiomyocytes Cellular Phenotypes After Myocardial Infarction. *Front. Cardiovasc. Med*, **8**, 750510.

Long, Y., Yang, Q., Xiang, Y., Zhang, Y., Wan, J., Liu, S., Li, N. & Peng, W. (2020) Nose to brain drug delivery - A promising strategy for active components from herbal medicine for treating cerebral ischemia reperfusion. *Pharmacol. Res.*, **159**, 104795.

McKenna, S., Garcia-Gutierrez, L., Matallanas, D. & Fey, D. (2021) BAX and SMAC regulate bistable properties of the apoptotic caspase system. *Sci. Rep.*, **11**, 3272.

Monroe, L.L., Armstrong, M.G., Zhang, X., Hall, J.V., Ozment, T.R., Li, C., Williams, D.L. & Hoover, D.B. (2016) Zymosan-Induced Peritonitis: Effects on Cardiac Function, Temperature Regulation, Translocation of Bacteria, and Role of Dectin-1. *Shock*, **46**, 723-730.

Nasiłowska-Barud, A., Zapolski, T., Barud, M. & Wysokinski, A. (2017) Overt and Covert Anxiety as a Toxic Factor in Ischemic Heart Disease in Women: The Link Between Psychological Factors and Heart Disease. *Med. Sci. Monit.*, **23**, 751-758.

Neri, M., Riezzo, I., Pascale, N., Pomara, C. & Turillazzi, E. (2017) Ischemia/Reperfusion Injury following Acute Myocardial Infarction: A Critical Issue for Clinicians and Forensic Pathologists. *Mediators Inflamm.*, **2017**, 7018393.

Obradovic, M., Sudar-Milovanovic, E., Gluvic, Z., Banjac, K., Rizzo, M. & Isenovic, E.R. (2023) The Na(+)/K(+)-ATPase: A potential therapeutic target in cardiometabolic diseases. *Front. Endocrinol.* (*Lausanne*), **14**, 1150171.

Oknińska, M., Maczewski, M. & Mackiewicz, U. (2022) Ventricular arrhythmias in acute myocardial ischaemia-Focus on the ageing and sex. *Ageing Res. Rev.*, **81**, 101722.

Pang, Y., Ma, M., Wang, D., Li, X. & Jiang, L. (2021) TANK Promotes Pressure Overload Induced Cardiac Hypertrophy via Activating AKT Signaling Pathway. *Front. Cardiovasc. Med.*, **8**, 687540.

Park, T.H., Lee, H.G., Cho, S.Y., Park, S.U., Jung, W.S., Park, J.M., Ko, C.N., Cho, K.H., Kwon, S. & Moon, S.K. (2023) A Comparative Study on the Neuroprotective Effect of Geopung-Chunghyuldan on In Vitro Oxygen-Glucose Deprivation and In Vivo Permanent Middle Cerebral Artery Occlusion Models. *Pharmaceuticals* (*Basel*), **16**, 596.

Peng, B., Xu, C., Wang, S., Zhang, Y. & Li, W. (2022) The Role of Connexin Hemichannels in Inflammatory Diseases. *Biology* (*Basel*), **11**, 237.

Promsan, S., Jaikumkao, K., Pongchaidecha, A., Chattipakorn, N., Chatsudthipong, V., Arjinajarn, P., Pompimon, W. & Lungkaphin, A. (2016) Pinocembrin attenuates gentamicin-induced nephrotoxicity in rats. *Can. J. Physiol. Pharmacol.*, **94**, 808-818.

Pun, R., Kim, M.H. & North, B.J. (2023) Role of Connexin 43 phosphorylation on Serine-368 by PKC in cardiac function and disease. *Front. Cardiovasc. Med.*, **9**, 1080131.

Qian, S., Wei, Z., Yang, W., Huang, J., Yang, Y. & Wang, J. (2022) The role of BCL-2 family proteins in regulating apoptosis and cancer therapy. *Front. Oncol.*, **12**, 985363.

Reilly, L. & Eckhardt, L.L. (2021) Cardiac potassium inward rectifier Kir2: Review of structure, regulation, pharmacology, and arrhythmogenesis. *Heart Rhythm*, **18**, 1423-1434.

Ren, F., Liu, X., Liu, X., Cao, Y., Liu, L., Li, X., Wu, Y., Du, S., Tian, G. & Hu, J. (2021) In vitro and in vivo study on prevention of myocardial ischemic injury by taurine. *Ann. Transl. Med.*, **9**, 984.

Singhanat, K., Apaijai, N., Jaiwongkam, T., Kerdphoo, S., Chattipakorn, S.C. & Chattipakorn, N. (2020) Melatonin as a therapy in cardiac ischemia-reperfusion injury: Potential mechanisms by which MT2 activation mediates cardioprotection. *J. Adv. Res*, **29**, 33-44.

Soto, M.E., Soria-Castro, E., Lans, V.G., Ontiveros, E.M., Mejia, B.I., Hernandez, H.J., Garcia, R.B., Herrera, V. & Perez-Torres, I. (2014) Analysis of oxidative stress enzymes and structural and functional proteins on human aortic tissue from different aortopathies. *Oxid. Med. Cell. Longev.*, **2014**, 760694.

Sutresno, A., Haryanto, F., Viridi & Arif, I. (2020) Influence Blocking by Gadolinium in Calcium Diffusion on Synapse Model: A Monte Carlo Simulation Study. *J. Biomed. Phys. Eng.*, **10**, 251-260.

Wang, J., Lu, L., Chen, S., Xie, J., Lu, S., Zhou, Y. & Jiang, H. (2020) Up-regulation of PERK/Nrf2/HO-1 axis protects myocardial tissues of mice from damage triggered by ischemia-reperfusion through ameliorating endoplasmic reticulum stress. *Cardiovasc. Diagn. Ther.*, **10**, 500-511.

Wang, R., Yang, M., Wang, M., Liu, X., Xu, H., Xu, X., Sun, G. & Sun, X. (2018) Total Saponins of Aralia Elata (Miq) Seem Alleviate Calcium Homeostasis Imbalance and Endoplasmic Reticulum Stress-Related Apoptosis Induced by Myocardial Ischemia/Reperfusion Injury. *Cell. Physiol. Biochem.*, **50**, 28-40.

Wang, X., Chen, J. & Huang, X. (2019) Rosuvastatin Attenuates Myocardial Ischemia-Reperfusion Injury via Upregulating miR-17-3p-Mediated Autophagy. *Cell Reprogram*, **21**, 323-330.

Wu, Y., Pan, N., An, Y., Xu, M., Tan, L. & Zhang, L. (2021) Diagnostic and Prognostic Biomarkers for Myocardial Infarction. *Front. Cardiovasc. Med.*, **7**, 617277.

Xie, Y., Gu, Z.J., Wu, M.X., Huang, T.C., Ou, J.S., Ni, H.S., Lin, M.H., Yuan, W.L., Wang, J.F. & Chen, Y.X. (2016) Disruption of calcium homeostasis by cardiac-specific over-expression of PPAR-gamma in mice: A role in ventricular arrhythmia. *Life Sci.*, **167**, 12-21.

Yang, J., Yin, H.S., Cao, Y.J., Jiang, Z.A., Li, Y.J., Song, M.C., Wang, Y.F., Wang, Z.H., Yang, R., Jiang, Y.F., Sun, J.P., Liu, B.Y. & Wang, C. (2018) Arctigenin Attenuates Ischemia/Reperfusion Induced Ventricular Arrhythmias by Decreasing Oxidative Stress in Rats. *Cell. Physiol. Biochem.*, **49**, 728-742.

Yang, Y., Jiang, K., Liu, X., Qin, M. & Xiang, Y. (2021) CaMKII in Regulation of Cell Death During Myocardial Reperfusion Injury. *Front. Mol. Biosci.*, **8**, 668129.

Zhang, J.Y., Yang, Z., Fang, K., Shi, Z.L., Ren, D.H. & Sun, J. (2017) Oleuropein prevents the development of experimental autoimmune myocarditis in rats. *Int. Immunopharmacol.*, **48**, 187-195.

Zhang, M., Wang, Z.Z. & Chen, N.H. (2023) Connexin 43 Phosphorylation: Implications in Multiple Diseases. *Molecules*, **28**, 4914.

Zhou, L., Sun, J., Yang, T., Wang, S., Shan, T., Gu, L., Chen, J., Wei, T., Zhao, D., Du, C., Bao, Y., Wang, H., Lu, X., Sun, H., Lv, M., et al. (2023) Improved methodology for efficient establishment of the myocardial ischemia-reperfusion model in pigs through the median thoracic incision. *J. Biomed. Res.*, **37**, 315-325.

Zhou, P., Xie, W., Luo, Y., Lu, S., Dai, Z., Wang, R., Sun, G. & Sun, X. (2018) Protective Effects of Total Saponins of Aralia elata (Miq.) on Endothelial Cell Injury Induced by TNF-alpha via Modulation of the PI3K/Akt and NF-kappaB Signalling Pathways. *Int. J. Mol. Sci.*, **20**, 36.